Memoirs of the Faculty of Science, Kyoto University, Series of Physics, Astrophysics, Geophysics and Chemistry, Vol. XXXX, No. 2, Article 3, 1998

Aseismic Blind-fault Movement before the 1995 Hyogo-ken Nanbu Earthquake Revealed from GPS Measurements

By

Shaorong ZHAO and Shuzo TAKEMOTO

Department of Geophysics, Graduate School of science, Kyoto University
Kyoto 606-8502, Japan

(Received January 9, 1998)

Abstract

By inversion of baseline changes and horizontal displacements observed with GPS (Global Positioning System) during 1990-1994, a possible blind-fault was recognized in Kinki-Shikoku region, Southwest Japan. The fault is characterized by a reverse dip-slip type (slip rate: 0.7 ± 0.2 m/year, at a layer of 17-26 km deep) with a length of 208 ± 5 km, a (down-dip) width of 9 ± 2 km, a dip-angle of $129\pm2°$, a bottom depth of 26 ± 2 km, and a strike direction of $40\pm2°$. An additional inversion analysis of the baseline changes observed by the permanent GPS array from 18 January to 31 December 1995 also indicated the activity of the blind-fault. Geological evidence of sub-faults close to the southwestern portion of the assumed fault and two historical earthquakes (M_L=7.0, 1789 and 6.4, 1955) which occurred near the fault partially supports the existence of the blind-fault in this region. The fact that almost no earthquakes ($M_L>2.0$) occurred at depth on the assumed fault plane suggests that the fault activity was mainly aseismic. Based on the parameters of the blind-fault estimated in this study, we calculated stress changes in this region. As a result, it is found that shear stress concentrated and increased by up to 2.1 bar/year at a depth of about 20 km around the epicentral area of the 1995 Hyogo-ken Nanbu earthquake ($M_L=7.2$), and that the earthquake hypocenter received a Coulomb failure stress of about 5.6 bar/year during 1990-1994. The results suggest that the 1995 Hyogo-ken Nanbu earthquake was possibly induced or triggered by aseismic fault movement. The significant activity of the blind-fault before and after the 1995 Hyogo-ken Nanbu earthquake might be transient, and may reflect the fault-like, macroscopic, ductile deformation in the lower crust. The fault-like activity in the lower crust may be responsible for the local stress concentration in this region.

1. Introduction

The 1995 Hyogo-ken Nanbu earthquake ($M_L=7.2$) occurred in the western part of the Osaka-Kobe megalopolis, Southwest Japan on January 17, 1995 (Figure 1). It caused 5,500 deaths and severe structural damage in the city of Kobe (e.g., Awata et al, 1996; Hashimoto et al., 1996). As a result of inversion analyses of coseismic horizontal displacements from GPS measurements, the earthquake fault (bold-line in Figure 1) is characterized by a right-lateral strike slip (1.3 ± 0.2 m) with a length of 32.8 ± 1.0 km, a width of 14.7 ± 1.0 km, a dip angle of $84.3°\pm1.0°$, a depth of 14.7 ± 0.5 km, and a strike direction of $48.8°\pm1.0°$ (Zhao and Takemoto, 1997). The earthquake fault geometry is consistent with failure under the regional stress field that dominates southwest Japan (Shiono, 1977). Distribution of horizontal strain in the area around the earthquake epicenter (about 900 km^2),

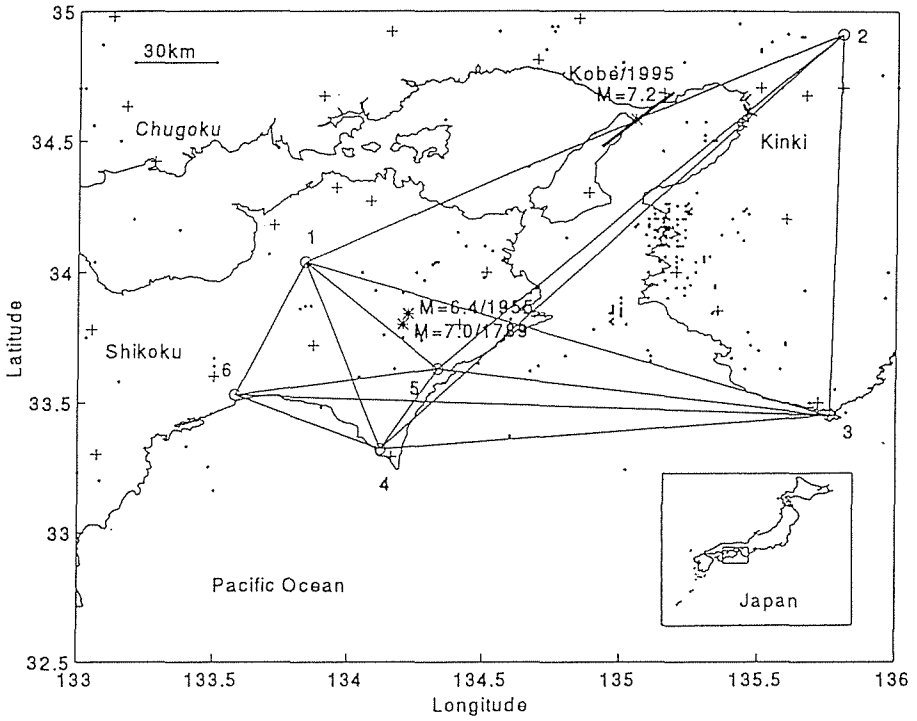

Fig. 1. Map showing the GPS stations (circles), baselines (thin solid-lines), the 1995 Hyogo-ken Nanbu earthquake fault (bold-line), and the epicenters (stars) of the 1789 ($M_L=7.0$) and 1955 ($M_L=6.4$) earthquakes. Also shown are the epicenters (dot) of microearthquakes ($M_L>2.0$) which occurred in the crust (<30 km deep) during 1 January-31 December 1994, and the seismic stations (plus sign) in this region. The average horizontal (latitude and longitude) standard error in microearthquake locations is ±2.0 km (Japan Meteorological Agency, 1996). The down-right inset is a sketch map of Japan in which the rectangle denotes the study area.

estimated from geodetic measurements over the last 100 years, shows that the north-south tensional strain was dominant, and that the east-west compressional strain was smaller than that in the other areas (ref. Geographical Survey Institute, 1986). Iio (1996), therefore, speculated that the normal stress on the Hyogo-ken Nanbu earthquake fault was reduced by the increase of tensional stress in the north-south direction that promoted the fault slip. Based on geological and geophysical data, Kanaori and Kawakami (1996) defined several microplates in Southwest Japan by linking large-scale active faults, and suggested that the 1995 Hyogo-ken Nanbu earthquake ruptured the central portion of one of the tectonic boundaries. In brief, the mechanism causing the intraplate earthquake is still unclear. GPS measurements during 1990-1994 detected significant horizontal deformation in the

Kinki-Shikoku region. In this study, we conduct an inversion analysis of the GPS baseline changes and horizontal displacements observed during 1990-1994 and investigate stress changes before the 1995 Hyogo-ken Nanbu earthquake in this region.

2. GPS Measurements during 1990-1994

The data used in this study are from the GPS campaign surveys of 1990-1994 in the Kinki-Shikoku region deployed by Kochi University and Disaster Prevention Research Institute of Kyoto University (Tabei et al., 1994; Date et al., 1995; Nakano, 1996).

In March 1990, the GPS survey started by using WM 102 receivers for about 5 days (Table 1). Daily observations were taken for 8 hours at a sampling interval of 60 seconds from satellites with an elevation angle >15 degrees. In January and March 1994, GPS observations were conducted with Ashtech Z-12 receivers for period of less than 3 days. Moreover, Ashtech Z-12 receivers were permanently installed at four stations (1, 2, 3 and 4 in Table 3) in April 1994 and since then, 24-hour-data with a sampling interval of 30 seconds have been continuously recorded. All data obtained during 1990-1994 were processed by the Bernese GPS software version 3.4. Satellite orbit information derived from broadcast ephemerides was used in processing the 1990 observations, whereas precise ephemerides were used in processing the 1994 observations. Station coordinates were calculated by using L_3 ionosphere-free linear combination of L_1 and L_2 carrier-phases together with the tropospheric zenith delay at each station every two hours. A weighted mean of the daily solutions was taken as the campaign solution, and standard deviations of the estimated coordinates in each campaign are defined as the square roots of the diagonal components of the covariance matrix. For the continuous measurements since October 1994, the weighted monthly mean was taken as a campaign solution (Tabei et al., 1996).

Linear trends of 14 baselines are listed in Table 2. Relative accuracy for observed baseline length is estimated to be 10^{-7} and 10^{-8} for the 1990 and 1994

Table 1. GPS surveys in Kinki-Shikoku region during 1990-1994

Survey	Session length	number of sessions	Receiver
March 6-10 1990	8 hours	5	WM 102
March 4-9 1991	8 hours	5	WM 102
January 4-5 1994	6 hours	7	Ashtech Z-12
March 8-10 1994	8 hours	8	Ashtech Z-12
April-December 1994	Continuous measurement		Ashtech Z-12

surveys, respectively. The average standard deviation for the baseline changes is estimated to be ±5.0 mm. As an example of length changes of baselines, Figure 2 shows the change on baseline No. 13 (ref. Table 2). From Figure 2 we see that long-term linear trend is dominant, although annual variations with small amplitudes are also presented. Horizontal displacement components are listed in Table 3. Figure 3 shows the horizontal station velocities with respect to the station 2 (Uji2) with error ellipses (one standard deviation). The precision of vertical components observed by the GPS surveys is about two or three times worse than that of the horizontal, and thus we did not use the vertical displacements in this study.

Table 2. Observed and predicted baseline changes (1990-1994)

Baseline No.	Stations	Observed (mm/year)	Predicted[1] (mm/year)
1	1-2	−10.7	−11.2
2	1-3	−16.8	−16.7
3	1-5	−19.9	−16.5
4	1-4	−12.2	−14.2
5	1-6	−3.8	−4.3
6	2-3	2.1	−3.1
7	2-5	−0.2	2.6
8	2-4	8.1	2.8
9	3-4	9.1	7.6
10	3-5	2.9	3.3
11	3-6	−3.3	−3.2
12	4-5	7.9	−0.8
13	4-6	−9.4	−9.0
14	5-6	−5.6	−7.8
σ(mm)		±5.0	±5.7

σ=average standard deviation;
[1]Computed using the fault parameters in Table 4.

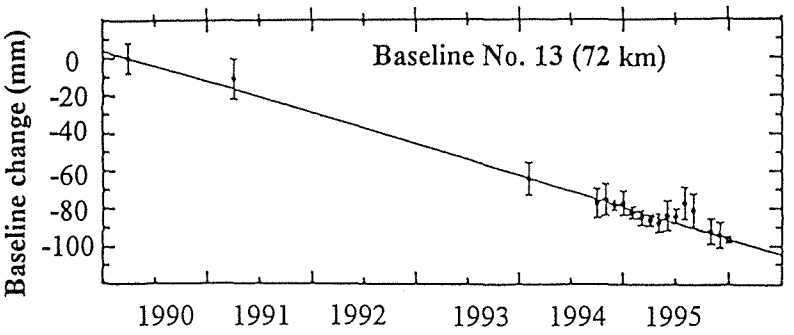

Fig. 2. Length change of baseline No. 13 (stations 4-6, ref. Table 2) during 1990-1995 (GPS campaign solutions are plotted with plus and minus one standard deviation (from Tabei et al., 1996). Note that the baseline changes shown here were resolved with respect to station 6 (which was taken as a fixed point), therefore the plot actually shows the motion of the station 4 relative to the station 6.

Table 3. Observed and predicted horizontal displacements (1990-1994)

Station No.	Observed (mm/year) W-E	S-N	Predicted[1] (mm/year) W-E	S-N	Predicted[2] (mm/year) W-E	S-N
1 (Iked)	10.0	4.0	10.1	2.8	8.4	4.5
2 (Uji2)	0.0	0.0	−1.4	0.5	−1.1	0.5
3 (Shio)	−10.0	−1.9	−7.3	3.7	−7.5	3.6
4 (Muro)	−20.0	7.0	−15.5	9.4	−18.0	11.2
5 (Kainan)	−11.0	11.0	−10.4	5.6	−13.2	7.1
6 (Kochi)	−6.0	15.0	−3.7	13.5	−4.6	15.0
σ (mm)	±3.5		±5.2		±5.3	

[1]From the inversion of observed baseline changes (computed using the fault parameters in Table 4); [2]From the inversion of observed horizontal displacements (computed using the fault parameters in Table 5); W-E = West-East; S-N = South-North; σ = average standard deviation of horizontal displacement components; Station 2 (Uji2) was taken as a fixed point in calculating the observed horizontal displacements.

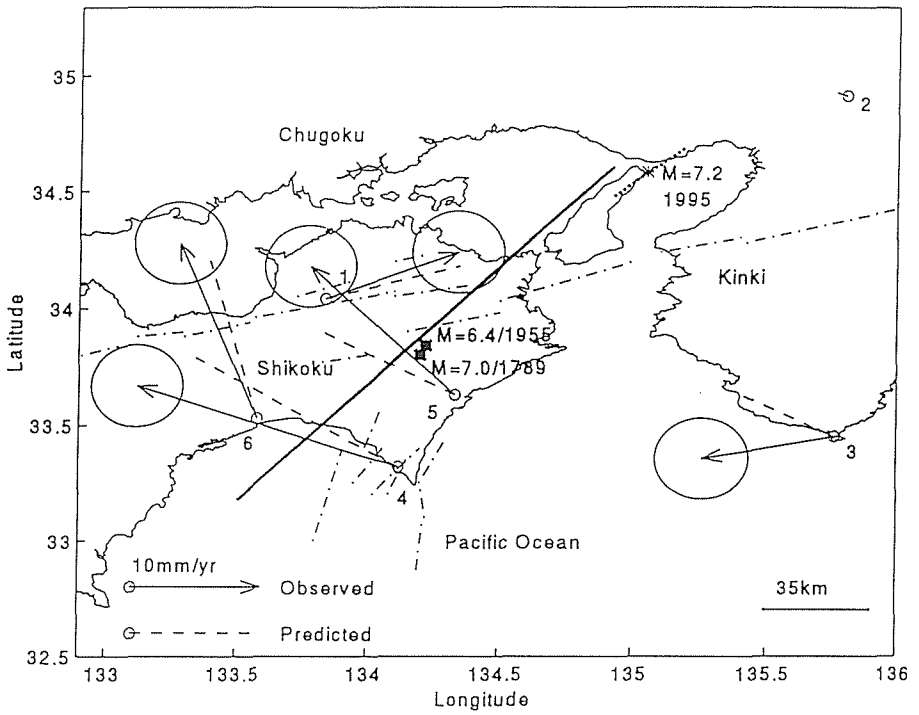

Fig. 3. Horizontal station velocities (site 2 fixed) during 1990-1994 with error ellipses (one standard deviation). Also shown are major geological faults (dash-dot lines), epicenters (stars) of earthquakes ($M_L \geq 6.0$), and the blind-fault found in this study (bold-line, the lower margin projected onto the ground surface). The broken line shows the fault segment of the 1995 Hyogo-ken Nanbu earthquake.

3. A Blind-fault Revealed by Inversion of Observed Baseline Changes and Horizontal Displacements

We investigate fault activity in this area by applying a non-linear inversion method (Zhao, 1995) to the observed baseline changes and horizontal displacements. On the basis of the expressions given by Okada (1992) for the deformations generated by a dislocation in an elastic half-space, nine parameters are adopted to delineate a fault segment (Table 4): L is the length of the fault segment, W is the fault width (down-dip), d is the (bottom) depth of the fault, δ is the dip angle of the fault, (λ, φ) are the geographical coordinates of the center (or source) of the fault, U_1, and U_2 are the strike- and dip-slip components, respectively, and α is the azimuth (or strike direction) of the fault (measured clockwise from the north). All of the nine parameters are taken as unknowns in the computations. The inversion computation is implemented by a designed search-program (Zhao, 1995). After searching for active fault segments in this region (about 300×250 km^2), we detected an active fault segment which fits the observations reasonably well (Figures. 3 and 4A).

The parameters of the fault model estimated from the inversion of observed baseline changes and horizontal displacements are listed in Tables 4 and 5, respectively. A disturbance analysis was performed to examine the stability of

Table 4. The blind-fault model estimated from the inversion of observed baseline changes during 1990-1994

Parameter		L (km)	W (km)	δ (°)	d (km)	α (°NE)	Source point λ	Source point φ	U_1 (m)	U_2 (m)	σ (mm)
Initial		180	10	140	14	53	134.00°	33.90°	−1.0	−1.0	
Final		208	9	129	26	40	134.21°	33.89°	−0.2	−0.7	
		±5	±2	±2	±2	±2	±5 km	±5 km	±0.2	±0.2	±5.7
Distur. I	Initial	160	5	150	14	50	134.10	33.70	−0.1	−0.3	
	Final	210	9	129	26	40	134.20	33.88	−0.2	−0.7	±5.9
Distur. II	Initial	190	10	120	20	45	134.10	33.80	−0.1	−0.5	
	Final	206	8	129	26	40	134.21	33.89	−0.2	−0.8	±5.8

Note: Initial = initial value; Final = final value; Distur. = Disturbance; λ = Longitude (E), φ = Latitude (N); and σ = the standard error of the inversion calculation.

Table 5. The blind-fault model estimated from the inversion of observed horizontal displacements during 1990-1994

Parameter		L (km)	W (km)	δ (°)	d (km)	α (°NE)	Source point λ	Source point φ	U_1 (m)	U_2 (m)	σ (mm)
Initial		180	10	140	24	50	134.10°	33.70°	−1.0	−1.0	
Final		202	6	123	26	42	134.21°	33.85	−0.3	−0.9	
		±10	±2	±2	±3	±5	±5 km	±5 km	±0.2	±0.3	±5.3
Distur. I	Initial	210	2	110	20	55	134.10	33.70	−0.3	−0.3	
	Final	195	7	130	24	41	134.22	33.84	−0.2	−0.6	±6.1
Distur. II	Initial	200	3	120	26	50	134.10	33.70	−0.7	−0.5	
	Final	213	7	127	24	40	134.23	33.86	−0.2	−0.8	±6.8

Ref. Table 4 for legends.

the inversion calculations. The inversion computations are rather stable and converge rapidly (Figure 4B). The standard error (±5.7 mm) of the inversion calculation for the baseline changes is close to that (±5.0 mm) of the observations. This suggests that the inversion computation is statistically acceptable.

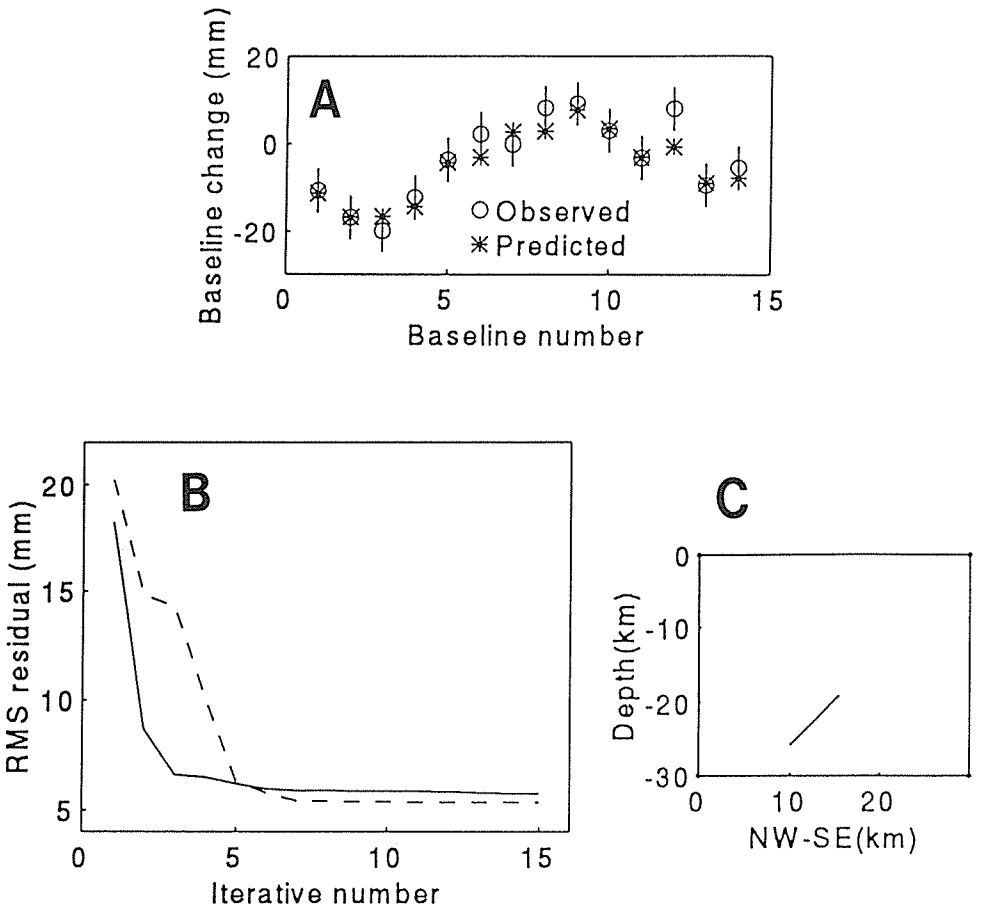

Fig. 4. (A) Observed (circle) and predicted (star) GPS baseline changes. The error bars represent one standard error of the observed baseline changes. The modelled GPS baseline changes (star) were computed with the parameters (Table 4) of the active fault model. Note the good fit between observations and predictions. The baseline numbers are (also see Figure 1): 1:1-2 (i.e., from point 1 to point 2), 2:1-3, 3:1-5, 4:1-4, 5:1-6, 6:2-3, 7:2-5, 8:2-4, 9:3-4, 10:3-5, 11:3-6, 12:4-5, 13:4-6, and 14:5-6. (B) The average RMS (root-mean-square) residual versus iterative number for inversion computation of the baseline changes (solid) and horizontal displacements (dashed), respectively. (C) Profile (running 130°NE, perpendicular to the fault strike direction) showing the active blind-fault at depth.

However, the standard deviation (±5.3 mm) of the inversion calculation for the horizontal displacements (Table 5) significantly exceeds that (±3.5 mm) of the observations, suggesting that there might be systematic errors in the horizontal displacements. Likely error sources are: (1) Distortions were introduced when assuming that the station 2 was fixed. From the predicted horizontal displacements in Table 3, we know that the station 2 was moving northwestward with a velocity of 1.5 mm/year. Thus, a systematic bias of about 1.5 mm exists in the observed displacements. (2) There might be some local deformations, which might not be interpreted by the active fault model.

We consider that the first error source seems more likely, in view of the differences between the observations and predictions (Table 3). In contrast, the results from the inversion of baseline changes were not affected by the selection of the reference (or fixed) point because the line length changes are independent of coordinate systems (Zhao, 1995). Therefore, we take the model from the inversion of the baseline changes (Table 4) as representative of the active fault during 1990-1994 in the study area. In addition, comparing the results in Tables 4 and 5, we know that the parameters of the active fault model estimated respectively from the baseline changes and horizontal displacements are almost identical, implying that the inversion computations are not very much affected by the small biases in the observations.

Moreover, results from an additional inversion analysis of the baseline changes observed by the nation-wide permanent GPS array during 18 January-31 December 1995 also revealed the presence of the active fault (ref. Appendix for a detailed analysis). The parameters of the active fault model estimated from the 1995 GPS data are also listed in Table 6. Overall, the parameters of the active fault model estimated from different data sets are consistent in general (ref. Table 6), except for a larger slip value ($U_2 = 1.6$ m) estimated from the 1995 data set and a deviation of about 13° in the fault strike direction (α). The baseline changes from the permanent GPS array were observed after the 1995 Hyogo-ken Nanbu earthquake. From Figure 3, we see that the earthquake ruptured a segment (broken line) near the northeastern end of the blind-fault (bold line). The observations from the permanent GPS array over the period 18 January-31

Table 6. Parameters of the active blind-fault estimated from different data sets

Parameter	L (km)	W (km)	δ (°)	d (km)	α (°NE)	Source point Long.	Lati.	U_1 (m)	U_2 (m)	σ (mm)
GPS data[1]	208	9	129	26	40	134.21°	33.89°	−0.2	−0.7	
(1990-1994)	±5	±2	±2	±2	±2	±5 km	±5 km	±0.2	±0.2	±5.7
GPS data[2]	202	4	123	26	42	134.21°	33.85°	−0.3	−0.9	
(1990-1994)	±5	±2	±2	±2	±2	±5 km	±5 km	±0.2	±0.2	±5.3
GPS data[3]	216	4	133	22	53	134.39°	33.80°	0.0	−1.6	
(1995)	±5	±2	±3	±3	±2	±4 km	±4 km	±0.1	±0.3	±5.2

[1]From the inversion of observed GPS baseline changes during 1990-1994; [2]From the inversion of observed horizontal displacements during 1990-1994; [3]From the inversion of baseline changes observed by the nation-wide permanent GPS array during 18 January-31 December 1995 (ref. Appendix).

December 1995 might have recorded some deformations caused by postseismic slip following the Hyogo-ken Nanbu earthquake (ref. Kato et al., 1996). Thus the fault parameters estimated from the inversion analysis of the 1995 observations have been probably affected by the postseismic effect. Despite the uncertainty, the GPS measurements during 1990-1994 and 1995 all suggest the existence of fault-like movement in the study area.

The possible fault segment during 1990-1994 was 208 ± 5 km long with a reverse dip-slip of 0.7 ± 0.2 m within a layer of about 17-26 km deep (Figures. 3 and 4C), though it does not clearly correspond with any known geological fault in the region, but is an unknown (blind) fault—not previously identified by geological investigations. Additional evidence from two historical earthquakes (M_L = 7.0, 1789; 6.4, 1955) and a series of faults striking northeast close to the southwestern portion of the assumed fault (see Figure 3; ref. Research Group for Active Faults in Japan, 1980) suggests that the present activity could be the reactivation of pre-existing faults. The epicenters (stars) of the 1789 $M_L = 7.0$ earthquake and the 1955 $M_L = 6.4$ earthquake are shown in Figures 1 and 3. At least, the evidence from the historical events, distribution of sub-faults as well as continuous GPS measurements over the period 18 January-31 December 1995 suggests that the blind-fault found in this study can not be caused by a data artefact or by systematic errors from the GPS data.

4. Stress Change before the 1995 Hyogo-ken Nanbu Earthquake Induced by Aseismic Movement of the Blind-fault

Figure 5 shows depth distribution of M >2.0 microearthquakes (circle) which

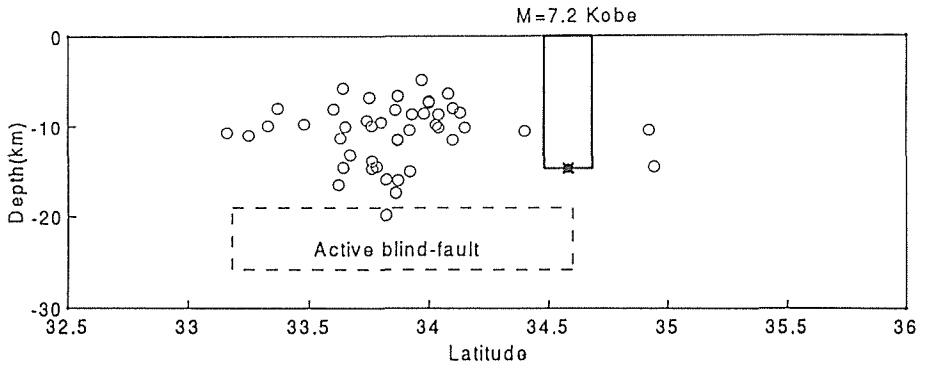

Fig. 5. Depth distribution of earthquakes (circle; $M_L > 2.0$ and depth < 30 km) which occurred during January-December 1994 within 40 km from the active fault trace. Also shown is the blind-fault (dashed-line rectangle) at depth (projected onto the profile running North-South direction; ref. Table 4 for the fault parameters). The bold-line rectangle represents the rupture plane of the 1995 Hyogo-ken Nanbu earthquake (Zhao and Takemoto, 1997).

occurred during the period of January-December 1994 within 40 km from the blind-fault trace (Japan Meteorological Agency, 1996). Microearthquakes which occurred outside this confined range (i.e., >40 km from the trace of the blind-fault) were not plotted onto the depth profile (Figure 5) because they might correspond to other mechanisms, rather than the activity of the blind-fault. The average standard error in microearthquake depths is estimated to be ± 2.5 km. The microearthquakes occurred largely within the upper crust (<20 km deep) and almost no earthquakes occurred on the fault plane at depth (dashed-line rectangle). This suggests that the fault activity was largely aseismic. In Figure 1, epicenters (dots) of the microearthquakes (depth <30 km, M_L> 2.0) during the period of January-December 1994 are also shown. The seismicity in the Kinki-Shikoku region before the 1995 Hyogo-ken Nanbu earthquake was at a level of normal background activity (Ando, 1995; Iio, 1996), which makes any attempt to establish a relationship between foreshocks and the main shock impossible. Nevertheless, it is plausible to assume that the blind-fault movement might have induced stress changes in this region. We evaluated stress changes in this area generated by the blind-fault movement. The parameters of the blind-fault estimated from the inversion of baseline changes of 1990-1994 (Table 4) were used in the computation. The shear stress changes (τ_{xy}) at a depth of 20 km in the study area are plotted in Figure 6A. It is found that there was significant shear stress concentration during 1990-1994 around the epicenter of the 1995 earthquake at a layer of 20 km depth, with the maximum shear stress change of about 2.1 bar/year (Figure 6A).

We also computed the change in the Coulomb failure function (CCFF) at the hypocenter of the 1995 Hyogo-ken Nanbu earthquake to assess whether the earthquake rupture segment was loaded to favour a rupture. The CCFF is defined by (Harris and Simpson, 1992; Reasenberg and Simpson, 1992; Stein et al., 1994):

$$\mathrm{CCFF}=\Delta\tau_s+\mu'\Delta\sigma_n \qquad (1)$$

where $\Delta\tau_s$ is the change in shear stress induced by movement of the blind-fault and resolved in the fault slip direction of the 1995 Hyogo-ken Nanbu earthquake and at the hypocenter, $\Delta\sigma_n$ is the change in normal stress (tension positive), and μ' is the apparent coefficient of friction containing the effects of pore pressure. Under the assumption that changes in fluid pressure were negligible, μ' can range between 0.0 and 0.8 with lower and higher values approximately representing higher and lower fluid pressure cases, respectively. Positive values of the CCFF indicate that a fault will be stressed to favour a rupture; negative values indicate movement away from failure.

Figure 6B shows changes in the Coulomb stress with depth at the epicenter of the 1995 Hyogo-ken Nanbu earthquake. The resultant Coulomb failure stress in the seismogenic layer (<20 km deep) is positive and increases from 0.0 to 5.6 bar with increasing depth from 0 to 15 km, but decreases below 15 km depth. The hypocenter of the 1995 earthquake (at a depth of about 15 km) has a CCFF value of about 5.6 bar. If the Coulomb failure stress increased with time at this rate during the 1990-1994 period, a failure stress accumulation of about 28.0 bar would be

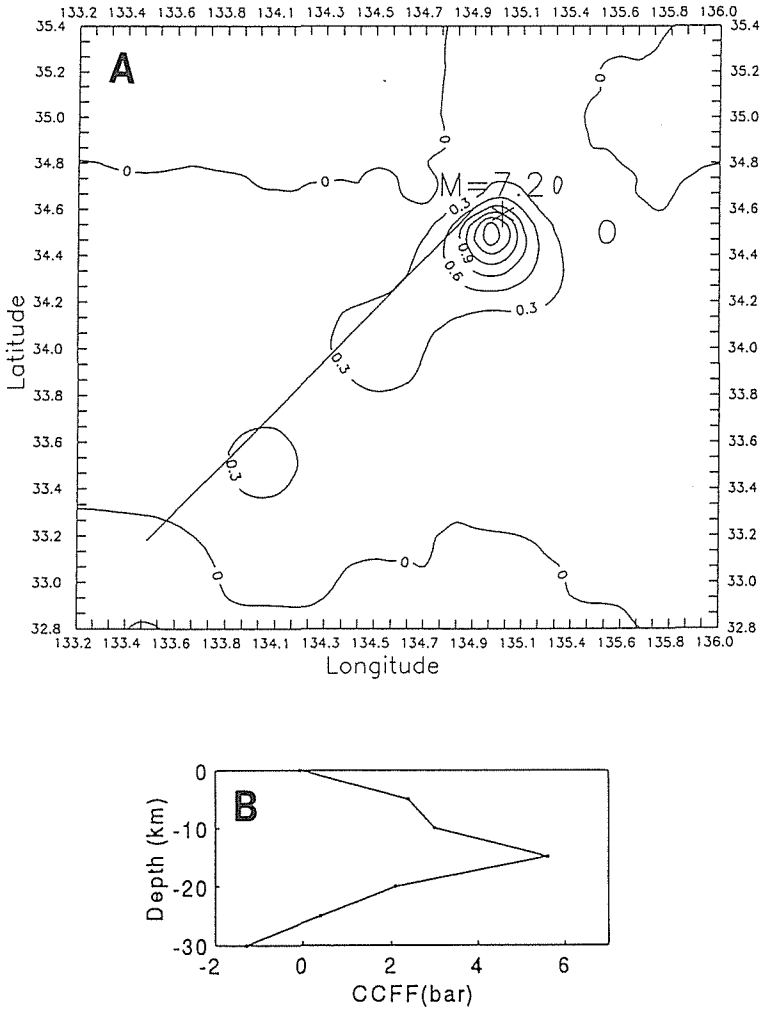

Fig. 6. Stress concentration caused by aseismic movement of the blind-fault before the 1995 Hyogo-ken Nanbu earthquake. (A) Shear stress change at a depth of 20 km; Also shown is the blind-fault segment (straight line) estimated from the GPS data. The star denotes the location of the 1995 Hyogo-ken Nanbu earthquake. The shear stress changes were computed with the fault parameters in Table 4. The contour interval is 0.3 bar. Note the significant shear stress concentration around the 1995 earthquake epicenter. (B) Change of Coulomb failure function (CCFF) at the site of the Hyogo-ken Nanbu earthquake plotted as a function of depth. The 1995 earthquake was represented as a vertical dislocation extending from the surface to a depth of 15 km (with a length of about 33 km and a strike direction of 49°NE). We examined results for the apparent coefficients of friction $\mu' = 0.2$, 0.5, and 0.8; the main pattern of the calculated CCFF is not changed and so we illustrate the results for $\mu' = 0.5$. Also note the maximum Coulomb failure stress at the hypocenter (about 15 km deep).

reached by 1995 at the hypocenter of the earthquake. Although this Coulomb failure stress accumulation might not be sufficient to produce the $M_L = 7.2$ earthquake, it could trigger the event if the earthquake fault was already near the limit of failure. From Figure 2, we see the linear trend in the baseline changes during this period, which partially justifies the above inference of the nearly linear increase in stress around the epicentral area during 1990-1994. Therefore, it seems likely that the 1995 Hyogo-ken Nanbu earthquake was induced or triggered by aseismic fault movements.

5. Summary and discussion

Based on the GPS observations during 1990-1994, we investigated fault activity in the Kinki-Shikoku region. Results from the inversion analysis of the horizontal displacements and baseline changes revealed a high-angle reverse blind-fault in the region (Figures 3 and 4C). The existence of the fault segment is supported partially by evidence from geological investigation of sub-faults close to the southwestern portion of the assumed fault and two earthquakes (M_L=7.0 and 6.4) which occurred in 1789 and 1955, respectively (Figures 1 and 3). Additional support for the present activity of the blind-fault comes from an inversion analysis of the baseline changes observed by the nation-wide permanent GPS array during 18 January-31 December 1995 (ref. Table 8 and Figure 8 in Appendix). Further stress analysis reveals that significant stress concentration occurred during 1990-1994 around the source area of the 1995 Hyogo-ken Nanbu earthquake (Figure 6). The shear stress at depth probably accumulated with time at a nearly linear rate in view of the linear trend of the baseline changes during 1990-1994 (ref. Figure 2), while the starting time of the stress build-up is unknown. It appears that there is a strong relationship between the site of the stress concentration and the hypocenter of the 1995 Hyogo-ken Nanbu earthquake. The earthquake hypocenter received a Coulomb failure stress up to 5.6 bar/year (Figure 6B), as induced by the activity of the blind-fault. Therefore, there is a possibility that the 1995 Hyogo-ken Nanbu earthquake was induced or triggered by aseismic movement of the blind-fault.

However, the deformation around the Shikoku island was usually interpreted as the results of the plate interaction at the Nankai trough (ref. Figure 7). Savage and Thatcher (1992) used a two-dimensional dislocation model to explain the vertical deformation in the region, and Ozawa (1997) used a backslip model to explain the horizontal deformation around the Shikoku island. These plate interaction models, though can partially interpret the deformation observed on the Shikoku island, could not directly account for the heterogeneous deformation in the Kinki-Shikoku region. The horizontal deformation observed in the Kinki-Shikoku region indicates that there might be block-motion between Chugoku, Shikoku, and Kinki (see Figure 8 in Appendix). In addition, the 1995 Hyogo-ken Nanbu earthquake is commonly believed to be an intraplate (crustal) earthquake, and the significant horizontal deformation observed before and after the earthquake in the

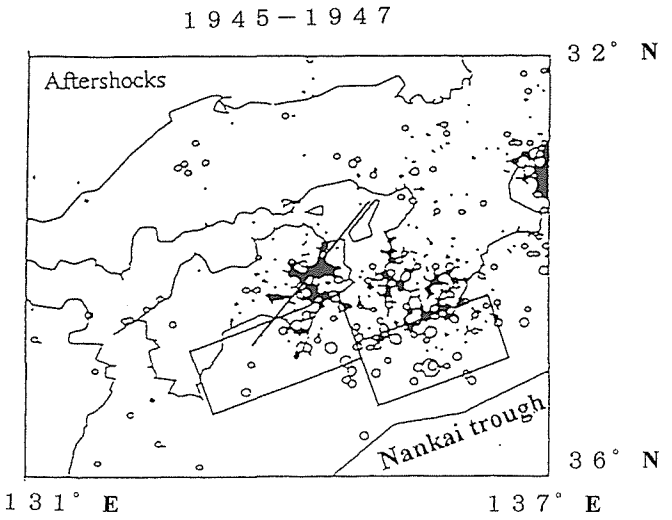

Fig. 7. Distribution of the earthquakes which occurred between 1945 and 1947 associated with the 1946 Nankaido earthquake (M_L = 8.2) (modified from Kimura and Okano, 1994). Also shown are the fault planes of the 1946 Nankaido earthquake estimated from geodetic data (fault parameters from Ando, 1982, RAN2). The solid-line denotes the blind-fault (lower margin) found in this study (ref. Table 4 for fault parameters).

Kinki-Shikoku region suggest that an intraplate mechanism might be responsible for the event. In this study, we focus on investigation of the relative motion between Chugoku, Shikoku, and Kinki around the site of the 1995 Hyogo-ken Nanbu earthquake. This is to assume implicitly that the effect of the plate interaction in the study area has been accommodated by the interaction (block-motion) between Chugoku, Shikoku, and Kinki. Although the relationship between the plate interaction and an intraplate earthquake is complicated, this study might offer an alternative way for analyzing the intraplate deformation near a subduction zone.

Our study was based on simple models using dislocations on rectangular surfaces in an elastic half-space (Okada, 1992). This model might not exactly describe the fault activity at depth, but we argue that the model can still represent the main characteristics of the fault-like motion in three-dimensions. The blind-fault detected in this study might not necessarily correspond to a geological fault, or even they are not directly comparable. A geological fault usually correspond to a time-scale of at least several millions of years, while the found blind-fault corresponds to a time-scale of several or tens of years. The magnitude of the slip-rate for the blind-fault may not necessarily be comparable with the slip-rate of a geological fault, because a geological slip-rate usually represents the surface-fault slip-rate, while the slip of the blind-fault found in this study occurred at a layer of 17-26 km deep, i.e., within the lower crust. The activity of the blind-fault revealed in this study might reflect the macroscopic deformation in the lower crust. The activity of the blind-fault might be transient, and may appear only several or tens of

years before an intraplate earthquake. The slip of the blind-fault in magnitude during the transient period may be comparable with the coseismic slip and afterslip of an earthquake.

Figure 7 shows the fault planes and aftershocks of the 1946 Nankaido earthquake ($M_L = 8.2$). Note that the southwestern portion of the blind-fault (solid-line) is overlapped by the concentration zone of the aftershocks in the eastern Shikoku. It seems that there is a relationship between the activity of the blind-fault today and the aftershock activity in the 1950's. A plausible interpretation may be that the 1946 Nankaido earthquake induced aftershocks as well as fault activity at the eastern Shikoku, and the gradual extension of the fault-like motion in the lower crust toward northeast resulted in stress localization and accumulation around the northeastern end of the blind-fault, which might ultimately serve as a trigging mechanism for the 1995 Hyogo-ken Nanbu earthquake. Finally, we noticed that this study has partially verified the triggering mechanism of the 1995 Hyogo-ken Nanbu earthquake suggested by Pollitz and Sacks (1997).

Appendix: Activity of the blind-fault revealed from the inversion analysis of the 1995 GPS data

Figure 8 shows the horizontal displacement (solid-arrows) observed by the permanent GPS array during 18 January-31 December 1995 (called GRAPES). The average accuracy of the horizontal displacement components is estimated to be ± 2 mm/yr. Details of the GPS data processing have been discussed by Miyazaki et al. (1996), and therefore will not be repeated here. We used this data set to examine whether the activity of the fault was still present in 1995. Since the Tsukuba station, ~ 400 km from the study area, was used as a (fixed) reference point in computing the horizontal displacements during 1995, it is not clear whether this reference point is suitable for determining the horizontal displacement field in Kinki-Shikoku region. To avoid possible systematic biases which might be introduced by an inadequate reference (coordinate) system, we choose to use the baseline changes in the subsequent inversion analysis, because the observed

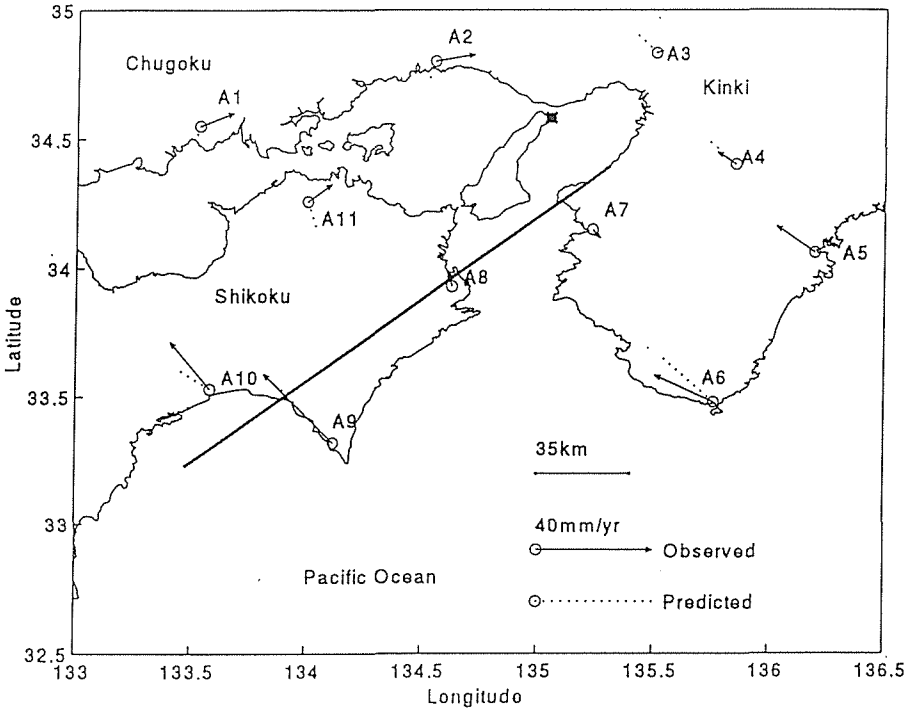

Fig. 8. Observed (arrows) and predicted (dotted lines) horizontal deformation during 18 January-31 December 1995 in the Kinki-Shikoku region. The average accuracy of the observed displacement components is less than ± 2 mm, and therefore the error ellipses are not plotted for brevity. The bold-line denotes the blind-fault (the lower margin projected onto the ground surface) estimated from the 1995 GPS data. The star denotes the epicenter of the 1995 Hyogo-ken Nanbu earthquake.

baseline changes are independent of any coordinate system and therefore will not be affected by the selection of a (fixed) reference point in the computation. A total of 27 baselines were used in this study and their distribution is shown in Figure 9 (dashed lines). The observed baseline changes are listed in Table 7 and shown in Figure 10A (circles). The average accuracy of the baseline changes is estimated to be ±5.0 mm. By inversion analysis of the baseline changes observed during 18 January-31 December 1995, the blind-fault is also detected, and its parameters are listed in Table 8. Figure 10B shows the iterative process of the inversion calculation. The standard deviation (±5.2 mm) of the inversion computation is close to that (±5.0 mm) of observations.

The predicted baseline changes are listed in Table 7 and shown in Figure 10A (stars). The horizontal displacements predicted by this fault model is shown in Figure 8 (dotted lines). From Figure 8, we can see that significant deviations exist between the observed and predicted horizontal displacement vectors at stations A1, A2, A3, and A11. It seems that there is a systematic rotation bias between the predictions and observations, e.g., for the vectors at stations A2, A6, A10, and A11. In view of the relatively good fit between the observed and predicted baseline

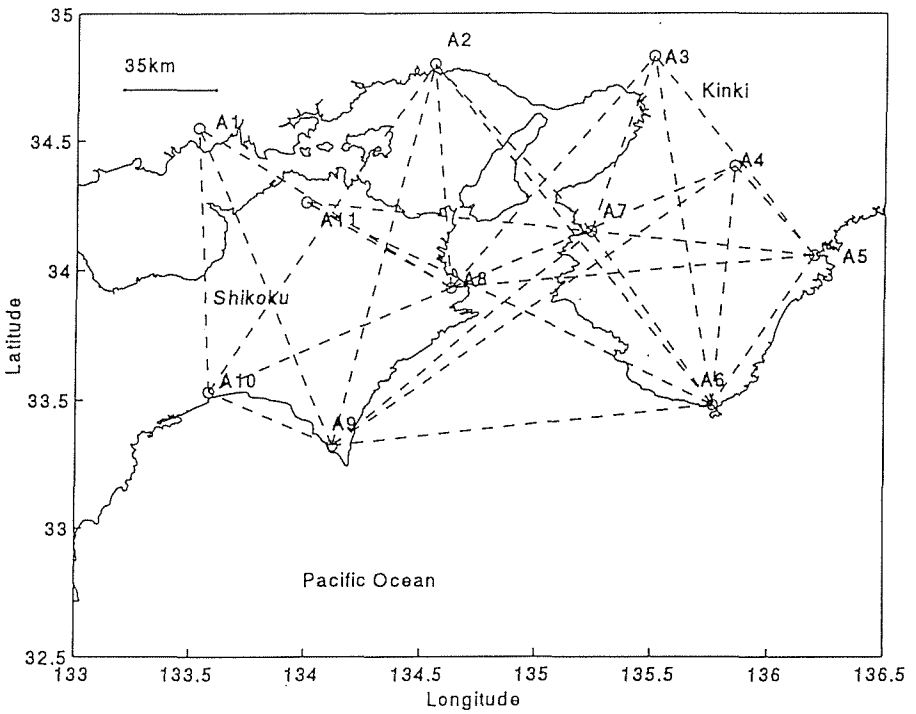

Fig. 9. Distribution of baselines (dashed) used in the inversion analysis (ref. Table 7 for the baseline changes).

Table 7. Observed and predicted baseline changes (18 January - 31 December 1995)

Baseline No.	Stations	Observed (mm)	Predicted[1] (mm)	Baseline No.	Stations	Observed (mm)	Predicted[1] (mm)
1	A5-A4	−7.8	−2.7	15	A10-A1	−11.9	−10.2
2	A5-A3	−14.7	−5.4	16	A10-A2	3.9	−5.2
3	A6-A4	−3.5	−5.6	17	A11-A7	−4.9	−3.7
4	A6-A3	−11.7	−9.3	18	A6-A11	−27.1	−29.7
5	A6-A7	−22.2	−20.5	19	A9-A7	4.3	4.2
6	A6-A2	−26.1	−25.0	20	A5-A7	−17.2	−15.0
7	A7-A2	−3.7	−3.4	21	A5-A6	3.6	−2.4
8	A7-A3	1.7	1.7	22	A5-A8	−11.6	−9.7
9	A8-A2	−4.2	−8.4	23	A6-A9	2.6	0.4
10	A8-A3	−3.0	0:2	24	A9-A4	3.8	1.1
11	A8-A1	−11.2	−4.9	25	A8-A4	−5.2	−4.2
12	A8-A11	−8.2	−12.0	26	A8-A10	7.1	6.0
13	A9-A1	−30.0	−25.7	27	A9-A10	−12.7	−11.1
14	A9-A2	−10.1	−18.5				

The average standard deviation is ± 5.0 and ± 5.2 mm for observations and predictions, respectively; [1]Computed using the fault parameters in Table 8.

Table 8. The blind-fault model estimated from the inversion of observed baseline changes (18 January-31 December 1995)

parameter	L (km)	W (km)	δ (°)	d (km)	α (°NE)	Source point λ	Source point φ	U_1 (m)	U_2 (m)	σ (mm)
Initial	200	10	120	15	50	134.20°	33.85	−0.4	−0.6	
Final	216	4	133	22	53	134.39°	33.80°	0.0	−1.6	
	±5	±2	±3	±3	±2	±4 km	±4 km	±0.1	±0.3	±5.2

Ref. Table 4 for legends.

changes (Table 7, Figure 10A), this possible systematic bias might exist in the observed horizontal displacement field, and does not affect the baseline changes. This might suggest that the reference (coordinate) system used in computing the nationwide horizontal deformation field might not be suitable for determining the local/regional deformation field. Despite this uncertainty, the inversion analysis of the 1995 GPS data also indicates the activity of the blind-fault in this region.

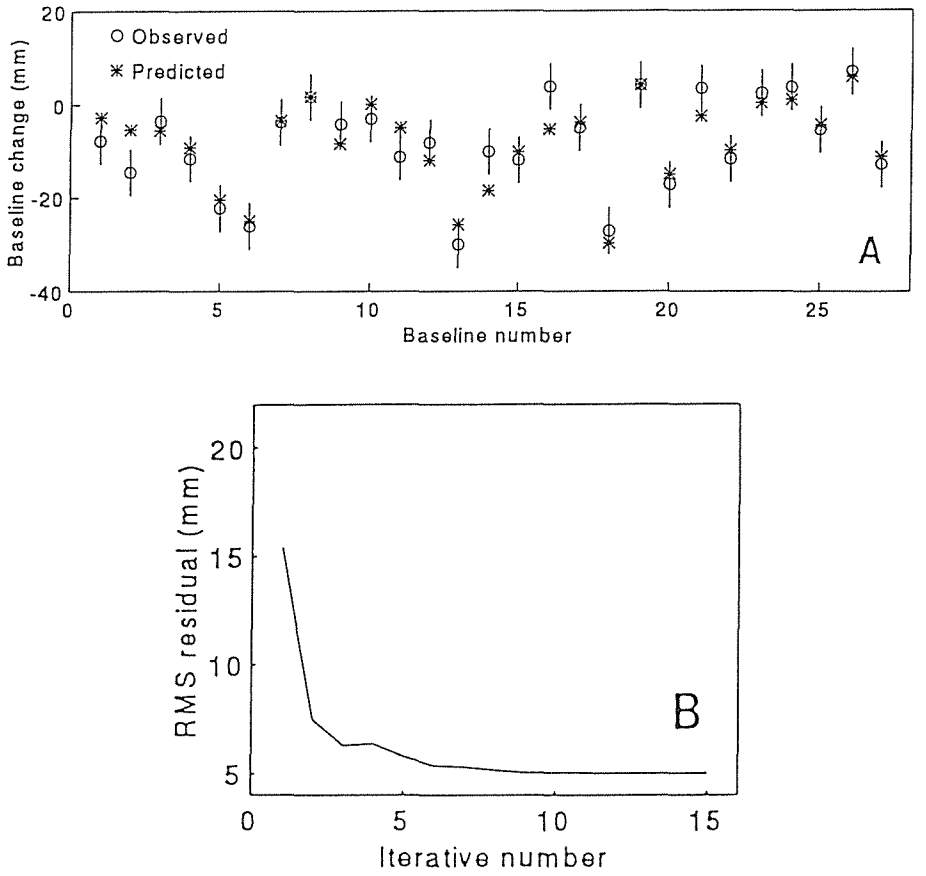

Fig. 10. (A) Observed (circle) and predicted (star) GPS baseline changes (18 January-31 December 1995). The error bars represent one standard error of the observed baseline changes. The modelled GPS baseline changes (star) were computed with the parameters (Table 8) of the active fault model. The baseline numbers are (also see Figure 9): 1:A5-A4 (i.e., from point A5 to point A4), 2:A5-A3, 3:A6-A4, 4:A6-A3, 5:A6-A7, 6:A6-A2, 7:A7-A2, 8:A7-A3, 9:A8-A2, 10:A8-A3, 11:A8-A1; 12:A8-A11; 13:A9-A1; 14:A9-A2; 15:A10-A1; 16:A10-A2; 17:A11-A7; 18:A6-A11; 19:A9-A7; 20:A5-A7; 21:A5-A6; 22:A5-A8; 23:A6-A9; 24:A9-A4; 25:A8-A4; 26:A8-A10; and 27:A9-A10. (B) The average RMS (root-mean-square) residual versus iterative number for inversion computation of the baseline changes (18 January-31 December 1995).

Acknowledgements

We thank Y. Okada for constructive comments on an earlier version of the manuscript, T. Tabei and Y. Kanaori for reprints, an anonymous reviewer for helpful comments, and the Japan Society for the Promotion of Science for a visiting fellowship (SZ).

References

Ando, M. (1982): A fault model of the 1946 Nankaido earthquake derived from tsunami data, Phys. Earth Planet. Inter., 28, 320-336.

Ando, M. (1995): Foreshocks, mainshocks, aftershocks and induced earthquakes of the 1995 Hyogo-ken Nanbu earthquake, Chikyu Monthly, Supp. 13. 18-29 (in Japanese).

Awata, Y., K. Mizuno, Y. Sugiyama, R. Imura, K. Shimokawa, K. Okumura, E. Tsukuba, and K. Kimura (1996): Surface fault ruptures on the northwest coast of Awaji island associated with the Hyogo-ken Nanbu earthquake of 1995, Japan, J. Seismol. Soc. Japan, 2, 49, 113-124 (in Japanese).

Date, Y., T. Tabei, and K. Hirahara (1995): Horizontal crustal deformation in Shikoku region, Southwest Japan, derived from GPS surveys: Results from 1990-1994 (Abstract), Japan Earth Planet. Sci. Joint Meeting, 122, March 27-30 (in Japanese).

Geographical Survey Institute (1986): Crustal movement in Kinki, Rep. Coord. Comm. Earthq. Pred., 34, 346-357 (in Japanese).

Harris, R.A. and Simpson, R.W. (1992): Changes in static stress on southern California faults after the 1992 Landers earthquake, Nature, 360, 251-254.

Hashimoto, M., T. Sagiya, H. Tsuji, Y. Hatanaka, and T. Tada (1996): Coseismic displacements of the 1995 Hyogo-ken Nanbu earthquake, J. Phys. Earth, 44, 255-279.

Iio, Y. (1996): A possible generating process of the 1995 southern Hyogo Prefecture earthquake: Stick of fault and slip on detachment, J. Seismol. Soc. Japan, 2, 49, 103-112 (in Japanese).

Japan, Meteorological Agency (1996): The Seismological Bulletin of the Japan, Meteorological Agency, January-December 1994.

Kanaori, Y. and S. Kawakami (1996): Microplate model and large inland earthquakes of Southwest Japan: Implications for generation of the 1995 M 7.2 Hyogo-ken-nanbu earthquake, J. Seismol. Soc. Japan, 2, 49, 125-139 (in Japanese).

Kato, T., Y. Kotake, S. Nakao, Y. Hirata, T. Chachin, F. Kimata, K. Yamaoka, T. Okuda, H. Kumagai, K. Hirahara, T. Nakano, T. Terashima, J.P.L. Catane, A. Kubo, T. Tabei, T. Iwabuchi, and T. Matsushima (1996): Post-seismic crustal deformation associated with the 1995 Hyogo-ken Nanbu earthquake derived from GPS observation: Preliminary analysis of Trimble data, J. Phys. Earth, 44, 287-299.

Kimura, S. and K. Okano (1994): Focal region of the 1946 Nankai earthquake inferred from the hypocenter distribution of mantle earthquakes in Shikoku, southwest Japan, Mem. Fac. Sci. Kochi Univ., 43, 79-89 (in Japanese).

Miyazaki, S., H. Tsuji, Y. Hatanaka, Y. Abe, A. Yoshimura, K. Kamada, K. Kobayashi, H. Morishita, and Y. Iimura (1996): Establishment of the nationwide GPS array (GRAPES) and its initial results on the crustal deformation of Japan,. Bull. Geograph. Surv. Inst., 42., 27-41.

Nakano, T. (1996): Postseismic deformation following the Hyogo-ken Nanbu earthquake observed with GPS, thesis, Graduate school of science., Kyoto Univ.

Okada, Y. (1992): Internal deformation due to shear and tensile faults in a half-space, Bull. Seismol. Soc. Am., 82, 1018-1040.

Ozawa, T. (1997): Interplate interaction in southwest Japan derived from GPS surveys, Master thesis, Kochi University, 1997.

Pollitz, F.F. and I.S. Sacks (1997): The 1995 Kobe, Japan, Earthquake: A long-delayed aftershock of the offshore 1944 Tonankai and 1946 Nankaido earthquake, Bull. Seism. Soc. Am., 87, 1-10.

Reasenberg, P.A. and Simpson, R.W. (1992): Response of regional seismicity to the static stress change produced by the Loma Prieta earthquake, Science 255, 1687-1690.

Research Group for Active Faults of Japan (1980): Active Faults in Japan: Sheet Maps and Inventories, University of Tokyo press, Tokyo (in Japanese).

Savage, J.C. and W. Thatcher (1992): Interseismic deformation at the Nankai Trough, Japan, subduction zone, J. Geophys. Res., 97, 11117-11135.

Shiono, K. (1977): Focal mechanisms of major earthquakes in southwest Japan and their tectonic significance, J. Phys. Earth, 25, 1-16.

Stein, R.S., King, G.S.P. and Lin, J. (1994): Stress triggering of the 1994 M = 6.7 Northridge,

California, earthquake by its predecessors, Science, 265, 1432-1435.
Tabei, T., Y. Date, K. Hirahara, and K. Nakamura (1994) : Horizontal crustal deformation in southeastern part of Shikoku, J. Seismol. Soc. Japan, 47, 303-310 (in Japanese).
Tabei, T., T. Ozawa, Y. Date, K. Hirahara, and T. Nakano (1996) : Crustal Deformation at the Nankai Subduction Zone, Southwest Japan, Derived from GPS Measurements, Geophys. Res. Lett., 23, 3059-3062.
Zhao, S. (1995) : Joint inversion of observed gravity and GPS baseline changes for the detection of the active fault segment at the Red River fault zone, Geophys. J. Int., 122, 70-88.
Zhao, S. and S. Takemoto (1997) : Fault geometry and rupture pattern of the 1995 Hyogo-ken Nanbu earthquake, Japan estimated by inversion of GPS data, J. Geod. Soc. Japan, 43, 33-43.